

Accepted Manuscript

Incorporation of a chiral *gem*-disubstituted nitrogen heterocycle yields an oxazolidinone antibiotic with reduced mitochondrial toxicity

Alexander W. Sun, Philip L. Bulterys, Michael D. Bartberger, Peter A. Jorth, Brendan M. O'Boyle, Scott C. Virgil, Jeff F. Miller, Brian M. Stoltz

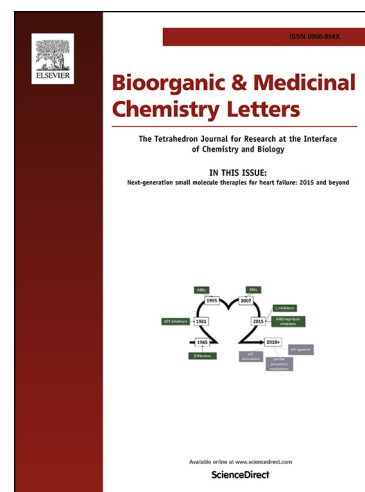
PII: S0960-894X(19)30469-X
DOI: <https://doi.org/10.1016/j.bmcl.2019.07.024>
Reference: BMCL 26565

To appear in: *Bioorganic & Medicinal Chemistry Letters*

Received Date: 7 April 2019
Revised Date: 8 July 2019
Accepted Date: 13 July 2019

Please cite this article as: Sun, A.W., Bulterys, P.L., Bartberger, M.D., Jorth, P.A., O'Boyle, B.M., Virgil, S.C., Miller, J.F., Stoltz, B.M., Incorporation of a chiral *gem*-disubstituted nitrogen heterocycle yields an oxazolidinone antibiotic with reduced mitochondrial toxicity, *Bioorganic & Medicinal Chemistry Letters* (2019), doi: <https://doi.org/10.1016/j.bmcl.2019.07.024>

This is a PDF file of an unedited manuscript that has been accepted for publication. As a service to our customers we are providing this early version of the manuscript. The manuscript will undergo copyediting, typesetting, and review of the resulting proof before it is published in its final form. Please note that during the production process errors may be discovered which could affect the content, and all legal disclaimers that apply to the journal pertain.

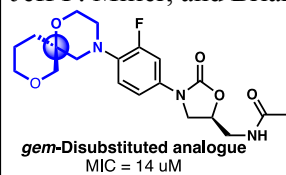


Graphical Abstract

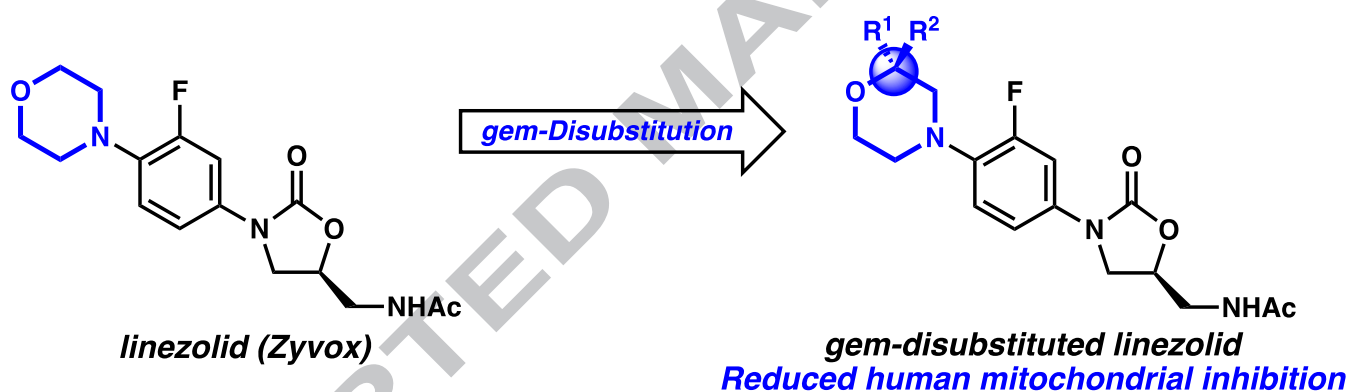
To create your abstract, type over the instructions in the template box below.
Fonts or abstract dimensions should not be changed or altered.

Incorporation of a chiral *gem*-disubstituted nitrogen heterocycle yields an oxazolidinone antibiotic with reduced mitochondrial toxicity

Alexander W. Sun, Philip L. Bulterys, Michael D. Bartberger, Peter A. Jorth, Brendan O'Boyle, Scott C. Virgil, Jeff F. Miller, and Brian M. Stoltz*



Leave this area blank for abstract info.





Incorporation of a chiral *gem*-disubstituted nitrogen heterocycle yields an oxazolidinone antibiotic with reduced mitochondrial toxicity

Alexander W. Sun,^a Philip L. Bulterys,^b Michael D. Bartberger,^a Peter A. Jorth,^a Brendan M. O'Boyle,^a Scott C. Virgil,^a Jeff F. Miller,^b and Brian M. Stoltz.^{a*}

^a The Warren and Katharine Schlinger Laboratory for Chemistry and Chemical Engineering, Division of Chemistry and Chemical Engineering, California Institute of Technology, Pasadena, California 91125, United States

^b Department of Microbiology, Immunology, and Molecular Genetics, University of California, Los Angeles, CA 90095, USA.

ARTICLE INFO

Article history:

Received

Revised

Accepted

Available online

Keywords:

Antibiotic

Mitochondria

Allylic Alkylation

Heterocycle

Linezolid

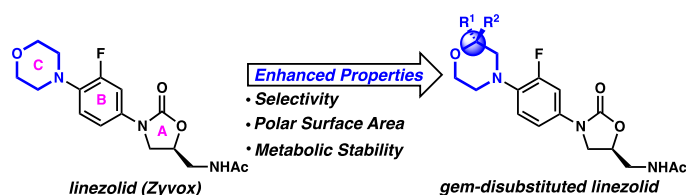
ABSTRACT

gem-Disubstituted *N*-heterocycles are rarely found in drugs, despite their potential to improve the drug-like properties of small molecule pharmaceuticals. Linezolid, a morpholine heterocycle-containing oxazolidinone antibiotic, exhibits significant side effects associated with human mitochondrial protein synthesis inhibition. We synthesized a *gem*-disubstituted linezolid analogue that when compared to linezolid, maintains comparable (albeit slightly diminished) activity against bacteria, comparable *in vitro* physicochemical properties, and a decrease in undesired mitochondrial protein synthesis (MPS) inhibition. This research contributes to the structure-activity-relationship data surrounding oxazolidinone MPS inhibition, and may inspire investigations into the utility of *gem*-disubstituted *N*-heterocycles in medicinal chemistry.

2019 Elsevier Ltd. All rights reserved.

gem-Disubstituted heterocycles are rare in small molecule pharmaceuticals. However, they exhibit the potential to further enhance the drug-like properties of small molecules (Figure 1). For example, *gem*-disubstitution significantly increases molecular complexity, which is correlated with decreased promiscuity and enhanced binding affinity to desired targets.¹⁻³ Furthermore, depending on the chemical identity of the substitutions, properties such as metabolic stability and polarity may also be altered (Figure 1).

Figure 1. Biological properties altered by hypothetical *gem*-disubstitution of the antibiotic linezolid



Given this potential, we sought to investigate the practical utility of *gem*-disubstituted heterocycles in bioactive small molecules. After surveying various *N*-heterocyclic drugs for cases in which physicochemical attributes could be improved by

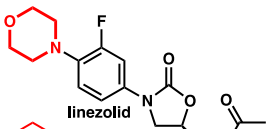
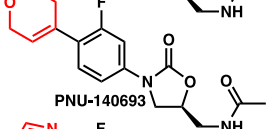
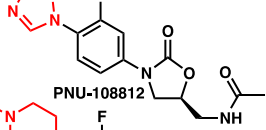
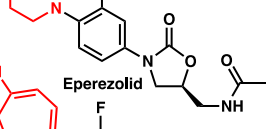
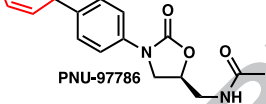
heterocyclic *gem*-disubstitution, we selected the morpholine-containing oxazolidinone antibiotic linezolid (Zyvox) (Figure 1). Approved by the FDA in 2001, linezolid inhibits bacterial peptide synthesis. Co-crystal structures show that linezolid binds to the A-site of the 50S subunit of the ribosome, interacting with an RNA pocket at the ribosomal peptidyl transferase center.^{4,5} This binding mode suggests that linezolid inhibits binding of aminoacyl tRNA. Linezolid and the recently approved oxazolidinone Tedizolid are important last resort antibiotics that are active against drug-resistant pathogens like methicillin-resistant *Staphylococcus aureus* (MRSA),⁶ vancomycin-resistant *Enterococcus faecalis* (VRE),⁷ and multi-drug resistant *Mycobacterium tuberculosis* (MDR-TB).⁸

Because the bacterial and human ribosomes are highly homologous, oxazolidinone antibiotics bind a commonly conserved site and thus also inhibit mitochondrial protein synthesis (MPS).⁹⁻¹² This off-target binding is thought to be responsible for linezolid's more significant side-effects, including myelosuppression, hyperlactatemia, and peripheral neuropathy.¹³ Other ribosome-targeting antibiotics such as clindamycin and chloramphenicol also exhibit corresponding myelotoxic side effects.^{14,15} If a structure-activity-relationship (SAR) could be determined for linezolid's mitochondrial binding ability, then new oxazolidinones could be designed with reduced MPS

inhibition. Indeed, reducing myelotoxic side effects while maintaining antibacterial potency is often cited as one of the greatest challenges in new oxazolidinone design.¹⁶

Fortunately, the modular structure of oxazolidinones enables chemical modification of all three rings, A, B, and C, facilitating SAR studies for mitochondrial ribosome binding (Figure 1). Some data have already been emerged. In 2006, McKee identified several oxazolidinones that more potently inhibit MPS yet display MIC values comparable to that of linezolid (Table 1).¹⁷ In these cases, the morpholine ring was replaced with other heterocycles, suggesting the C-ring may be the greatest determinant of MPS inhibition. In spite of these initial results, there are no known reports of a potent oxazolidinone featuring reduced MPS inhibition.

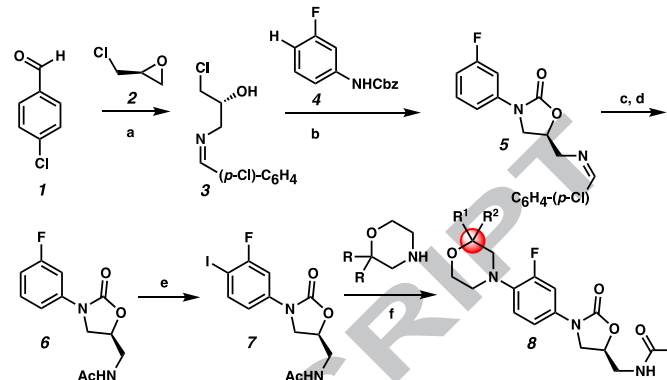
Table 1. MIC and MPS IC₅₀ values for linezolid analogues

	MIC ^a	IC ₅₀ ^b
	2	12.8
	1	0.95
	4	1.7
	2	4.2
	2	0.83

^a MIC (μg/mL) for *S. aureus* JC9213. ^b IC₅₀ (μg/mL) for mitochondrial protein synthesis

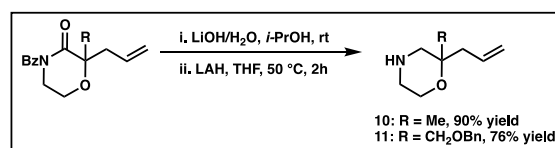
We thus initiated a medicinal chemistry project seeking to modify the morpholine C-ring of linezolid with the goal of reducing MPS inhibition. Importantly, crystal structure studies note that the morpholine ring does not make significant interactions with the binding pocket, suggesting that the ring can be modified without compromising binding.⁵ Because increased molecular complexity is associated with reduced ligand promiscuity, we hypothesized that *gem*-disubstitution of the morpholine ring could potentially increase selectivity for the bacterial ribosome and reduce off-target side effects such as MPS inhibition (Figure 1). To test this hypothesis, we began by identifying a modular route to enable the synthesis of a library of *gem*-disubstituted linezolid analogs (Scheme 1). Cross-coupling of a *gem*-disubstituted morpholine with aryl halide **7** was identified as an efficient route. Thus, aryl halide **7** was synthesized by adapting a patent procedure.¹⁸ Briefly, (*S*)-epichlorohydrin (**2**) was coupled with 4-chlorobenzaldehyde (**1**) and ammonia to give imine **3**. To forge the oxazolidinone intermediate **5**, imine **3** was then subjected to a base-catalyzed coupling reaction with carbamate **4**,¹⁹ which itself was made by addition of benzyl chloroformate to 3-fluoroaniline. Finally, imine hydrolysis, *N*-acetylation, and iodination provided the aryl iodide **7**. **7** was cross-coupled under copper-catalyzed Ullmann

conditions²⁰ with a variety of *gem*-disubstituted morpholines resulting in linezolid analogues **12-19** (Figure 2). Notably, this synthetic route will facilitate future efforts to modify the C morpholine ring of linezolid.



Scheme 1. Synthesis of *gem*-disubstituted linezolid analogues via Cu-catalyzed Ullmann coupling. a. (*S*)-epichlorohydrin, NH₄OH (aq), THF, 40 °C, 12 h, 55% yield; b. LiOt-Bu, CH₂Cl₂, rt to 40 °C, 87% yield; c. 1N HCl, H₂O/EtOAc; d. Ac₂O, CH₂Cl₂, 96% yield over 2 steps; e. NIS, TFA, rt, 92% yield; f. Substituted morpholine **11a-p**, CuBr (10 mol %), BINOL (20 mol %), K₃PO₄, DMF, 80 °C.

Two analogues **13** and **14** were prepared using substituted morpholines **10** and **11**, which were synthesized via a decarboxylative alkylation protocol and subsequent deprotective and reductive transformations (Scheme 2).²⁰ Other analogues including the *gem*-dimethyl compound **12** and spiro compounds **15-19** were prepared from commercially available di-substituted morpholines. We note that all analogs were synthesized as racemates.



Scheme 2. Synthesis of *gem*-disubstituted morpholines by benzoyl cleavage and reduction of morpholinone decarboxylative alkylation products

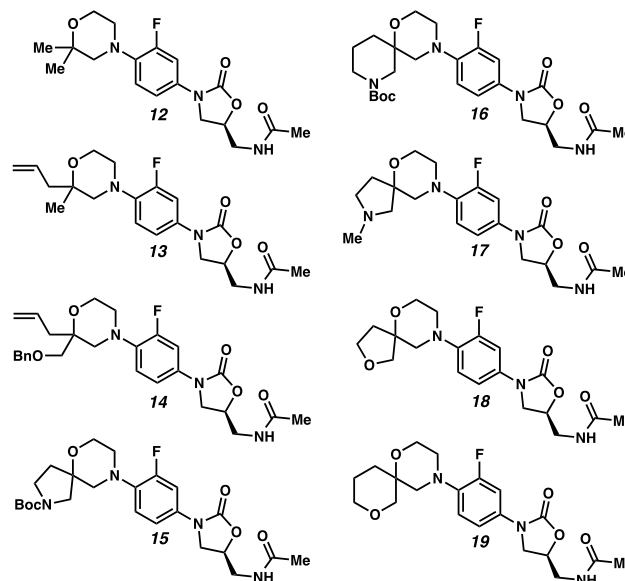
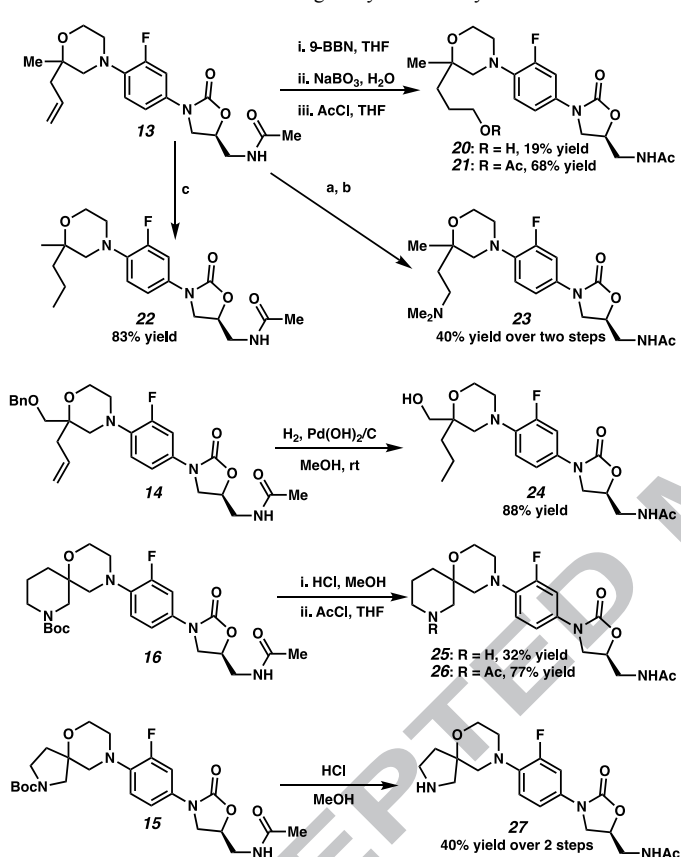


Figure 2. *gem*-Disubstituted linezolid analogues synthesized via Ullmann coupling

Additionally, analogues synthesized via Ullmann coupling could be further derivatized (Scheme 3). Taking advantage of the

versatile allyl handle of **13**, hydroboration-oxidation afforded hydroxyl analogue **20**, which could be acetyl-protected to give analogue **21**. Additionally, a Lemieux–Johnson oxidation provided the aldehyde intermediate, which was reductively aminated with dimethylamine to provide analogue **23**. Catalytic hydrogenation afforded the reduced analogue **22**. Similarly, the benzyloxy analogue **14** could also be hydrogenated using catalytic Pd(OH)₂ on carbon to provide the hydroxyl analogue **24**. Finally, Boc-spiro compound **16** was deprotected using HCl resulting in spiro piperidine **25**; subsequent acetyl protection gave **26**. Similarly, acid-catalyzed Boc-cleavage of **15** afforded spiro pyrrolidine **27**.

Scheme 3. Additional analogues synthesized by derivatization



With a diverse set of *gem*-disubstituted linezolid analogues in hand, we proceeded with broth microdilution assays against *S. aureus* to determine minimum inhibitory concentration (MIC) values (Table 2). The initial three compounds, **12**, **13**, **24**, were noticeably less potent than linezolid, suggesting that bulky alkyl di-substitution on the morpholino ring reduces activity. Similarly, bulky hydroxyl-substituted analogue **20** and protected alcohols **21** and **14** were also inactive. In contrast, hydroxyl analogue **24** retained a moderate amount of activity, displaying 48% growth inhibition at the maximal tested concentration of 6 µg/mL. The amine-bearing derivatives, **23**, **27**, **17**, and **25**, featuring methylamino, dimethyl amino, and spiroamine functionalities, were uniformly inactive up to 32 µg/mL concentrations. Interestingly, when the basic nitrogen of **25** was masked as an amide as in **26**, an 18% growth inhibition at the maximal tested concentration of 6 µg/mL was achieved, suggesting that positively charged substituted morpholines are not tolerated. Finally, we were excited to observe increased growth inhibition when the spirofuran **18** and spiro tetrahydropyran **19** analogues were tested, with **19** displaying the greatest potency of all analogues examined. Since stereoisomers often exhibit differing

biological activity, we used chiral HPLC to obtain both diastereomers of **19**, and then assigned their absolute stereochemistry using vibrational circular dichroism (VCD) and optical rotation calculations, both of which were in agreement (see supporting information for details of synthesis and purification) (Figure 3). Notably a eudysmic difference between the two diastereomers **19a** and **19b** was observed, with the more active diastereomer **19a** displaying an MIC of 6 µg/mL, roughly sixfold less potent than linezolid (Table 2).

Table 2. MIC values against ATCC 8235-4 (MSSA) or ATCC 43300 (MRSA)

Compound	MIC (µg/mL)	Compound	MIC (µg/mL)
Linezolid	1 ^{a,b}	23	> 32 ^b
12	8 ^a	27	> 32 ^b
13	16 ^a	17	> 32 ^b
22	16 ^a	25	> 32 ^b
20	> 32 ^a	26	6 µg/mL: 18% inhib. ^c
21	> 32 ^b	18	6 µg/mL: 65% inhib. ^c
14	> 32 ^b	19	7 ^b
24	6 µg/mL: 48% inhib. ^{b,c}	19a	6 ^b
		19b	9 ^b

MIC: the lowest concentration of molecule preventing visible growth. [a] Tested against *S. aureus* ATCC 43300. [b] Tested against *S. aureus* ATCC 8235-4. [c] 6 µg/mL was the maximal concentration tested.

We further investigated the bioactivity of **19a** against other strains of *S. aureus*, determining the MIC values to be consistent against a range of MSSA and MRSA strains (Table 3).

Table 3. MIC values of lead analogue **19a** against various *S. aureus* strains

Strain	Linezolid MIC (µg/mL)	19a MIC (µg/mL)
<i>S. aureus</i> ATCC 8235-4	1	6
<i>S. aureus</i> 43300	1	5
<i>S. aureus</i> 29213	1	5
<i>S. aureus</i> 25923	1	5

We next examined the pharmacokinetic properties of **19a** and **19b**, determining most properties were slightly lower but comparable to that of linezolid (Table 4). For instance, **19a** and **19b** demonstrated slightly lower aqueous solubility and stability at low pH. Microsomal stability for was also lower than that of linezolid, perhaps due to the metabolic susceptibility of the tetrahydropyran ring. Initial safety data including cytotoxicity and cytochrome P450 isoform inhibition were satisfactory. One interesting difference was MPS inhibition, in which linezolid displayed a relatively potent 8 µM IC₅₀. In contrast, **19a** displayed an IC₅₀ value of 30 µM. This finding correlates with the relative MIC values of linezolid and **19a**; in this case, MPS inhibition is also roughly three-fold less potent, suggesting that the spiro tetrahydropyran ring of **19a** maintains moderate binding

affinity to the bacterial ribosome while reducing inhibition of the mitochondrial ribosome.

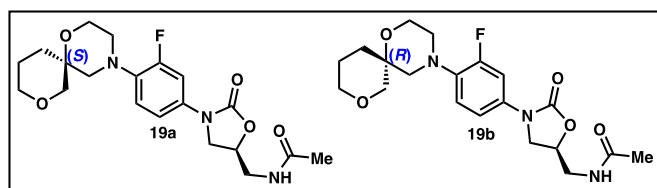


Figure 3. Diastereomers of analogue **19**. Absolute configuration of the spirocyclic stereocenter determined by both VCD and optical rotations (See supporting information for details).

Table 4. Pharmacokinetic properties, inhibitory activity, and physicochemical properties

	Linezolid	19a	19b
Aq. Solubility ($\mu\text{g/mL}$)	>67.47	>52.15	>48.49
Stability at gastric pH (% remaining 24 h)	98%	94%	89%
$t_{1/2}$ microsomes (min) ^a	>216.8	170.0	128.3
Cytotoxicity EC_{50} (μM) ^b	>30	> 30	>30
CYP inhibition (μM) ^c	>100	> 100	>100
Mt protein synthesis inhibition IC_{50} (μM) ^d	8.19	30	> 30

^a Metabolic stability performed with mouse liver microsomes

^b Cytotoxicity against HepG2 cells using CellTiter Glo

^c Measured against CYP1A2, 2C9, 2C19, 2D6, 3A4

^d MitoBiogenesis In-Cell ELISA assay for COXI and SDH-A mitochondrial proteins

In conclusion, we identified a *gem*-disubstituted morpholine analogue of linezolid bearing a spirotetrahydropyran substitution,

Acknowledgments

A.W.S. and B.M.S. conceived of the project. A.W.S., B.M.O., M.D.B., and S.C.V. performed experimental chemistry. P.L.B., P.A.J., and WuXi AppTec performed biological assays. M.D.B. performed VCD experiments. A.W.S., P.L.B., M.D.B., P.A.J., B.M.O., J.F.M., and B.M.S. wrote the manuscript.

The NIH-NIGMS (R01GM080269), Caltech, the Paul and Daisy Soros Foundation, and the UCLA-Caltech Medical Scientist Training Program are thanked for support of our research program. (Grants R01GM080269 to B.M.S., F30GM120836 and T32GM008042 to A.W.S., F30AI118342, T32GM008042 and P.D. Soros Fellowship to P.L.B.). Dr. David VanderVelde is thanked for assistance with structural assignments via NMR analysis. Dr. Justin Hilf is thanked for helpful discussions. Professor Dianne K. Newman is thanked for MIC testing. The CO-ADD is thanked for MIC testing. The UCLA Microbiology Laboratory is thanked for providing bacterial strains.

References and notes

(1) Vitaku, E.; Smith, D. T.; Njardarson, J. T. Analysis of the Structural Diversity, Substitution Patterns, and Frequency of Nitrogen

19a, that displays slightly reduced potency compared to linezolid against various *S. aureus* strains while also having reduced mitochondrial inhibition. These results contribute to the existing SAR of MPS inhibition (Table 1). Although the mitochondrial and bacterial ribosomes share homology, they have structural differences that may be exploited to design molecules with reduced selectivity for the mitochondrial ribosome.⁹ Our research further contributes to the body of data suggesting that the morpholine ring is a key structural component whose modification can reduce mitochondrial inhibition while maintaining bacterial ribosome inhibition. Continued efforts are needed to identify a molecule as potent as linezolid but with reduced MPS inhibition. This ability of *gem*-disubstituted heterocycles to alter selectivity for a target such as the bacterial ribosome highlights one of the many useful properties of heterocyclic substitution. In recent years, powerful methods have been developed to stereoselectively synthesize *gem*-disubstituted heterocycles. For instance, our laboratory has pioneered the development of Pd-catalyzed decarboxylative asymmetric allylic alkylation methodologies to synthesize a range of *gem*-disubstituted lactams of ring size 5 to 7.^{21–24} Such lactams can be deprotected and reductively transformed into the corresponding *gem*-disubstituted *N*-heterocycles. These methods and others to access *gem*-disubstituted heterocycles will greatly enable the investigation of the medicinal utility of such heterocycles. Efforts, such as those underway in our laboratory to incorporate *gem*-disubstituted heterocycles into other small molecule scaffolds will undoubtedly shed light on the broader medicinal utility of *gem*-disubstituted heterocycles.

Heterocycles among U.S. FDA Approved Pharmaceuticals. *J. Med. Chem.* **2014**, *57*, 10257–10274.

- (2) Lovering, F.; Bikker, J.; Humblet, C. Escape from Flatland: Increasing Saturation as an Approach to Improving Clinical Success. *J. Med. Chem.* **2009**, *52*, 6752–6756.
- (3) Lovering, F. Escape from Flatland 2: Complexity and Promiscuity. *Med. Chem. Commun.* **2013**, *4*, 515–519.
- (4) Ippolito, J. A.; Kanyo, Z. F.; Wang, D.; Franceschi, F. J.; Moore, P. B.; Steitz, T. A.; Duffy, E. M. Crystal Structure of the Oxazolidinone Antibiotic Linezolid Bound to the 50S Ribosomal Subunit. *J. Med. Chem.* **2008**, *51*, 3353–3356.
- (5) Wilson, D. N.; Schluenzen, F.; Harms, J. M.; Starosta, A. L.; Connell, S. R.; Fucini, P. The Oxazolidinone Antibiotics Perturb the Ribosomal Peptidyl-Transferase Center and Effect TRNA Positioning. *PNAS* **2008**, *105*, 13339–13344.
- (6) Ender, M.; McCallum, N.; Adhikari, R.; Berger-Bächi, B. Fitness Cost of SCCmec and Methicillin Resistance Levels in *Staphylococcus aureus*. *Antimicrob. Agents Chemother.* **2004**, *48*, 2295–2297.
- (7) Gonzales, R. D.; Schreckenberger, P. C.; Graham, M. B.; Kelkar, S.; DenBesten, K.; Quinn, J. P. Infections Due to Vancomycin-Resistant Enterococcus Faecium Resistant to Linezolid. *The Lancet* **2001**, *357*, 1179.
- (8) Schechter, G. F.; Scott, C.; True, L.; Raftery, A.; Flood, J.; Mase, S. Linezolid in the Treatment of Multidrug-Resistant Tuberculosis. *Clin. Infect. Dis.* **2010**, *50*, 49–55.
- (9) Leach, K. L.; Swaney, S. M.; Colca, J. R.; McDonald, W. G.; Blinn, J. R.; Thomasco, L. M.; Gadwood, R. C.; Shinabarger, D.; Xiong, L.; Mankin, A. S. The Site of Action of Oxazolidinone Antibiotics in Living Bacteria and in Human Mitochondria. *Mol. Cell* **2007**, *26*, 393–402.

- (10) Sharma, M. R.; Koc, E. C.; Datta, P. P.; Booth, T. M.; Spremulli, L. L.; Agrawal, R. K. Structure of the Mammalian Mitochondrial Ribosome Reveals an Expanded Functional Role for Its Component Proteins. *Cell* **2003**, *115*, 97–108.
- (11) Greber, B. J.; Bieri, P.; Leibundgut, M.; Leitner, A.; Aebersold, R.; Boehringer, D.; Ban, N. The Complete Structure of the 55S Mammalian Mitochondrial Ribosome. *Science* **2015**, *348*, 303–308.
- (12) Amunts, A.; Brown, A.; Toots, J.; Scheres, S. H. W.; Ramakrishnan, V. The Structure of the Human Mitochondrial Ribosome. *Science* **2015**, *348*, 95–98.
- (13) Narita, M.; Tsuji, B. T.; Yu, V. L. Linezolid-Associated Peripheral and Optic Neuropathy, Lactic Acidosis, and Serotonin Syndrome. *Pharmacotherapy* **2007**, *27*, 1189–1197.
- (14) Duewelhenke, N.; Krut, O.; Eysel, P. Influence on Mitochondria and Cytotoxicity of Different Antibiotics Administered in High Concentrations on Primary Human Osteoblasts and Cell Lines. *Antimicrob. Agents Chemother.* **2007**, *51*, 54–63.
- (15) Li, C.-H.; Cheng, Y.-W.; Liao, P.-L.; Yang, Y.-T.; Kang, J.-J. Chloramphenicol Causes Mitochondrial Stress, Decreases ATP Biosynthesis, Induces Matrix Metalloproteinase-13 Expression, and Solid-Tumor Cell Invasion. *Toxicol. Sci.* **2010**, *116*, 140–150.
- (16) Shaw, K. J.; Barbachyn, M. R. The Oxazolidinones: Past, Present, and Future. *Ann. N. Y. Acad. Sci.* **2011**, *1241*, 48–70.
- (17) McKee, E. E.; Ferguson, M.; Bentley, A. T.; Marks, T. A. Inhibition of Mammalian Mitochondrial Protein Synthesis by Oxazolidinones. *Antimicrob. Agents Chemother.* **2006**, *50*, 2042–2049.
- (18) Imbordino, R.; Perrault, W.; Reeder, M. Process for Preparing Linezolid. WO/2007/116284, October 19, 2007.
- (19) Yang, B.; Shi, L.; Wu, J.; Fang, X.; Yang, X.; Wu, F. Microwave-Assisted Expeditious Synthesis of 5-Fluoroalkyl-3-(Aryl/Alkyl)-Oxazolidin-2-Ones. *Tetrahedron* **2013**, *69*, 3331–3337.
- (20) Mahy, W.; Leitch, J. A.; Frost, C. G. Copper Catalyzed Assembly of N-Aryloxazolidinones: Synthesis of Linezolid, Tedizolid, and Rivaroxaban. *Eur. J. Org. Chem.* **2016**, 1305–1313.
- (21) Sun, A. W.; Hess, S. N.; Stoltz, B. M. Enantioselective Synthesis of Gem-Disubstituted N-Boc Diazaheterocycles via Decarboxylative Asymmetric Allylic Alkylation. *Chem. Sci.* **2019**, *10*, 788–792.
- (22) Behenna, D. C.; Liu, Y.; Yurino, T.; Kim, J.; White, D. E.; Virgil, S. C.; Stoltz, B. M. Enantioselective Construction of Quaternary N-Heterocycles by Palladium-Catalyzed Decarboxylative Allylic Alkylation of Lactams. *Nat. Chem.* **2012**, *4*, 130–133.
- (23) Numajiri, Y.; Jiménez-Osés, G.; Wang, B.; Houk, K. N.; Stoltz, B. M. Enantioselective Synthesis of Dialkylated N-Heterocycles by Palladium-Catalyzed Allylic Alkylation. *Org. Lett.* **2015**, *17*, 1082–1085.
- (24) Korch, K. M.; Eidamshaus, C.; Behenna, D. C.; Nam, S.; Horne, D.; Stoltz, B. M. Enantioselective Synthesis of α -Secondary and α -Tertiary Piperazin-2-Ones and Piperazines by Catalytic Asymmetric Allylic Alkylation. *Angew. Chem. Int. Ed.* **2015**, *54*, 179–183.

Supplementary Material

Supplementary material that may be helpful in the review process should be prepared and provided as a separate electronic file. That file can then be transformed into PDF format and submitted along with the manuscript and graphic files to the appropriate editorial office.

